Proceedings of CONF-FMCE 2025 Symposium: Semantic Communication for Media Compression and Transmission
DOI: 10.54254/2755-2721/2025.GL24471

Investigation of the Synergistic Activation of Estrogen Receptors ERα and ERβ by DIBP and MIBP: A Molecular Docking Study Based on AutoDock

Zhijian Wang

College of Resources and Environment, Huazhong Agricultural University, Wuhan, China
1261251918@qq.com

Abstract. This study aims to investigate the synergistic activation effects and molecular mechanisms of diisobutyl phthalate (DIBP) and its metabolite monoisobutyl phthalate (MIBP) on estrogen receptors ERα and ERβ under combined exposure. Using AutoDock 4.2.6, molecular docking of the ligand-binding domains (LBDs) of ERα and ERβ is performed to analyze binding free energy (ΔG), key interaction sites, and spatial complementarity under single and combined treatments. The results show significant synergistic effects of DIBP and MIBP on both ERα and ERβ, which is hypothesized to result from the specific spatial complementarity of DIBP and MIBP in the receptors and the additive effect of binding energies, thereby significantly enhancing their synergistic activation of ERα and ERβ. Overall, DIBP-MIBP preferentially activate ERβ (ΔG=-9.058) more potently than ERα (ΔG=-7.73) through a two-site synergistic mechanism, suggesting that mixed exposure may enhance endocrine-disrupting effects on non-reproductive systems. This highlights the insufficient attention paid to the synergistic effects of PAEs metabolites and provides a basis for establishing receptor subtype-specific exposure limits. Given the scarcity of research on mixed exposure and the incomplete understanding of underlying mechanisms, and because molecular docking results solely reflect receptor binding capacity, the conclusions are inferred from binding energies and require validation by in vitro/in vivo experiments to demonstrate functional effects.

Keywords: phthalates, estrogen receptors, molecular docking simulation, synergistic effect

1. Introduction

Phthalates (PAEs), as plasticizers, are widely present in plastic products, accounting for approximately 70% of all plasticizer consumption, and are extensively used in food packaging, medical devices, and other applications. It is reported that the exposure level of PAEs in the Chinese population ranges from 23 to 159 μg/kg·bw·d, posing significant risks to human health [1]. Diisobutyl phthalate (DIBP), a common derivative of PAEs, has been detected in some farmland soils and vegetables in China. As a typical environmental estrogen, DIBP is rapidly hydrolyzed in vivo into the monoester metabolite monoisobutyl phthalate (MIBP), which exhibits enhanced polarity and prolonged half-life, potentially undergoing accumulative metabolic transformation

DOI: 10.54254/2755-2721/2025.GL24471

through enterohepatic circulation. Studies from Antwerp University Hospital in Belgium have shown that detection rates of DIBP and MIBP in scalp hair of premature infants exceed 90%, yet the biological effects of their combined exposure remain unclear [2]. PAEs in the environment often exist as mixtures, yet current research predominantly focuses on single compounds, with their synergistic toxicity mechanisms remaining undefined [3]. Studies have shown that co-exposure to DIBP and MIBP may enhance ER activation effects through synergistic action, and traditional single-compound risk assessment models may underestimate actual health risks [4].

Studies on residential environments in Shihezi City have confirmed that the co-occurrence rate of DIBP and MIBP in dustfall is as high as 90%. Experiments have shown that MIBP enhances the sustained activation effect of DIBP on ERα/ERβ by prolonging the half-life of ERβ (from 2.3 hours to 4.7 hours) [5] Additionally, as receptors for the estrogen estradiol, ERα and ERβ are frequently used in docking experiments with PAE-like substances to simulate interactions and investigate toxicity, which is crucial for improving risk assessment models for mixed PAE pollutants [6]. AutoDock predicts the binding modes, binding free energy (ΔG), and key interaction sites between small-molecule ligands and biological macromolecules through computational simulation, providing a theoretical basis for understanding the molecular recognition mechanism [7]. This study uses AutoDock simulation to reveal: 1) whether DIBP-MIBP synergistically activates ERα/ERβ through spatial complementary binding; and 2) whether the synergistic effect is related to the conformational plasticity of the receptor ligand-binding domain (LBD) [8]. The results serve as a molecular mechanism basis for subtype-specific risk assessment of mixed PAEs. Subsequent validation using molecular dynamics simulation (GROMACS) is required [9].

2. Methodology

2.1. Materials preparation

The following procedures were employed to prepare materials and conduct molecular docking simulations in a rigorous and reproducible manner.

To acquire the crystal structures of ERα and ERβ ligand-binding domains (LBDs), the RCSB Protein Data Bank (PDB) was queried using relevant keywords. Structures originating from Homo sapiens with a resolution equal to or better than 2.5 Å were selected. Priority was given to complexes co-crystallized with natural ligands such as estradiol, as these structures provide biologically relevant conformations [10]. The selected PDB files were further processed using AutoDock Tools (MGLTools), wherein all water molecules were removed and polar hydrogen atoms were added. The processed structures were then saved in PDBQT format, and the coordinates of the active sites were recorded for subsequent docking studies.

Small-molecule ligands were obtained from the PubChem database. For each compound, the three-dimensional conformer was downloaded in SDF format. Using Avogadro software, the SDF files were imported, water molecules were removed, and polar hydrogen atoms were added. The resulting structures were exported in PDB format and subsequently converted to PDBQT format using AutoDock Tools to prepare them for docking analysis.

2.2. Individual docking simulation

Individual molecular docking simulations were carried out using AutoDock. Each small molecule was docked to its respective receptor independently. Grid parameters for the receptor were defined to ensure coverage of the core active site, with center coordinates set at x=38.709, y=11.947, and

DOI: 10.54254/2755-2721/2025.GL24471

z=30.490, and a grid size of 56×56×52Å [11]. Following preprocessing with AutoGrid, docking simulations were performed with both ligands and receptors treated flexibly. Each docking run was repeated to enhance reliability, and the following parameters were recorded: binding energy, hydrogen bond interactions, and hydrophobic contacts [12].

2.3. Combined docking simulation

For combined docking simulations, DIBP and MIBP were selected as ligands, and ERα and ERβ served as receptors. The receptor grid parameters used were identical to those applied in individual docking simulations. Initial setup files were saved in TXT format. Based on the single-ligand docking protocol, modifications were introduced to accommodate a second ligand and increase the number of docking runs to 15. AutoDock Vina was then employed to perform the simulations. Upon completion, the conformation exhibiting the lowest binding energy was selected for further analysis. The corresponding binding energies and hydrogen bond interaction sites were systematically documented and analyzed to elucidate the potential binding mechanisms.

3. Results analysis

This study unveils the synergistic activation mechanism of DIBP-MIBP on ERα/ERβ through molecular docking simulations. DIBP and MIBP bind to distinct sites on ERα, such as ARG330 and ARG473, located at the HE and HH12 regions, respectively. Both sites are involved in the selective binding of estrogen analogs (e.g., SERMs). Tamoxifen disrupts the active conformation of AF-2 by interfering with ARG473, whereas the stabilizing effect of ARG330 may partially counteract this disruption [13]. For ERβ, DIBP and MIBP also target different yet functionally critical sites.

3.1. ERα

DIBP and MIBP exhibit a binding mode characterized by moderate spatial competition within the ERα ligand-binding domain (LBD), leading to a markedly enhanced binding affinity in the combined docking scenario. The resulting binding energy (ΔG= –7.73 kcal/mol) is substantially lower than that observed for the individual ligands when docked separately (DIBP: –4.68 kcal/mol; MIBP: –5.75 kcal/mol), suggesting potential synergistic effects in their co-binding behavior.

Table 1: ERα binding to ligands

ligand	Maximum binding energy (kcal/mol)	Maximum number of hydrogen bonds
DIBP	-4.68	3
MIBP	-5.75	4
DIBP and MIBP	-7.73	

As illustrated in Table 1, the maximum binding energy of DIBP is approximately 1 kcal/mol higher than that of MIBP, with a similar number of hydrogen bonds. However, in the combined action with ligands, the maximum binding energy is significantly reduced by 2 kcal/mol compared to MIBP, indicating an enhanced toxicity effect.

DOI: 10.54254/2755-2721/2025.GL24471

Table 2: Comparison table of DIBP and MIBP binding to ERα

ligand	Binding Region	Key Binding Residues	Functional Effect
DIBP	H3-H5 helical region	ARG330,ALA307	Stabilizes hydrophobic pocket, weak AF-2 activation
MIBP	H11-H12 junction	ARG472/473/476	Strong AF-2 conformational locking, enhanced transcriptional activity

Through the comparison of experimental results, Table 2 was obtained. Based on the number of hydrogen bonds and their interaction strength, the binding affinity of DIBP was speculated to be at a moderate level. At the binding site ARG330, two hydrogen bonds are formed between the side-chain hydrogen atoms (HE, HH22) and the oxygen atom of DIBP, anchoring the ligand core. Additionally, binding to the ALA307 site forms one hydrogen bond between the backbone oxygen atom and the oxygen atom of DIBP, stabilizing the edge of the hydrophobic pocket. The binding site is located in the H3-H5 helical region of the ERα LBD, adjacent to the AF-2 domain (H12 helix).

Due to one additional hydrogen bond and the involvement of multiple arginine residues, its binding energy is speculated to be stronger than that of DIBP: four hydrogen bonds formed at ARG472/ARG473/ARG476 sites constitute an "arginine cluster," significantly enhancing the polar complementarity between the ligand and LBD. The binding at the HH21 site of ARG472 additionally contributes a salt bridge or strong polar interaction, potentially inducing conformational changes in the H12 helix. The binding site is located at the junction of the H11-H12 helices, directly influencing AF-2 coactivator recruitment [14].

3.2. ERβ

DIBP and MIBP form a spatially complementary binding mode in the ERβ ligand-binding domain (LBD), resulting in a significantly lower binding energy (ΔG= -9.06 kcal/mol) in combined action than that of single ligands (DIBP alone: -6.28 kcal/mol; MIBP: -5.24 kcal/mol). This indicates a higher potential toxic hazard to humans.

mode	affinity (kcal/mol)	dist from best mode rmsd l.b.	rmsd u.b.
1	-9.058	0	0
2	-9.05	2.637	5.439
3	-9.025	15.38	17.16
4	-8.958	2.018	3.327
5	-8.918	15.37	16.92
6	-8.862	14.96	16.81
7	-8.845	15.56	17.19
8	-8.739	1.233	2.27
9	-8.718	1.906	3.007
10	-8.587	15.63	17.38
11	-8.514	15.42	17.3
12	-8.448	15.2	18.23
13	-8.34	15.62	17.5
14	-8.28	2.235	5.613
15	-8.172	14.99	17.09

Figure 1: Results of 15 simulations of co-binding of DIBP and MIBP

DOI: 10.54254/2755-2721/2025.GL24471

As shown in Figure 1, Mode 1 exhibits the strongest binding capacity with an affinity of -9.058 kcal/mol, indicating the most stable binding to the target. The affinities of all modes range from -9.058 to -8.172 kcal/mol, showing an overall trend of gradual weakening. Measured by "distance from the best mode (RMSD lower bound)", there are two distinct patterns as follows:

Low-deviation modes (<5 Å):

Modes 2 (2.637 Å), 4 (3.327 Å), 8 (2.27 Å), and 14 (5.613 Å) have structures highly similar to the best mode, likely representing fine-tuned conformations at the same binding site.

High-deviation modes (>15 Å):

Modes 10 (17.38 Å), 11 (17.3 Å), 12 (18.23 Å), and 13 (17.5 Å) exhibit substantially different structures, potentially representing entirely different binding sites or conformational inversions.

Table 3: ERα binding to ligands

ligand	Maximum binding energy (kcal/mol)	Maximum number of hydrogen bonds
DIBP	-6.28	2
MIBP	-5.24	4
DIBP and MIBP	-9.058	
ligand Binding Region		

As can be seen from Table 3, the difference in maximum binding energy between DIBP and MIBP is 1 kcal/mol, and the number of hydrogen bonds of MIBP is many. The maximum binding energy after synergistic binding is about 3 kcal/mol lower compared to DIBP. The results show that MIBP and DIBP synergize significantly more on ERβ than on ERα.

Table 4: Comparison table of DIBP and MIBP binding to ERβ

ligand	Binding Region	Key Binding Residues	Functional Effect
DIBP	H3-H5 helical region	ARG454,ASN457	Hydrophobic-dominated, weak AF-2 activation
MIBP	H11-H12 junction	HIS394,LYS395,GLN393	Polar network-driven, strong AF-2 conformational locking

Analysis of experimental results shows that(Table 4):

DIBP binds to the H3-H5 helical region of the ERβ LBD (ligand-binding domain), which serves as the core hydrophobic pocket for ERβ-ligand interactions. At the ARG454 site, hydrogen bonds are formed between the side-chain hydrogen atom (HE) and the oxygen atom of DIBP, stabilizing the ligand binding pose. The ASN457 site further enhances polar complementarity through a hydrogen bond between its HD21 group and DIBP's oxygen atom. Notably, DIBP binding does not significantly induce conformational changes in the H12 helix (AF-2 domain), leading to weak coactivator recruitment capacity. While hydrophobic interactions maintain local stability of the LBD, overall receptor activation efficiency remains low [15].

In contrast, MIBP binds to the H11-H12 helical junction, directly modulating the conformation of the AF-2 domain. The primary binding sites and their functions are:

HIS394/LYS395: Forms dual hydrogen bonds with MIBP via backbone amines, anchoring the ligand's polar groups.

GLN393: The side-chain HE21 group hydrogen bonds with MIBP, enhancing binding specificity.

LYS395: The side-chain HZ2 group stabilizes the ligand site through electrostatic interactions.

MIBP binding induces the H12 helix to fold toward the ligand, significantly exposing the coactivator-binding interface. With a network of four hydrogen bonds, MIBP exhibits lower binding free energy and activation efficiency approaching that of endogenous estrogens.

DOI: 10.54254/2755-2721/2025.GL24471

3.3. Results and discussion

The comparison of the binding sites reveals that DIBP and MIBP exhibit distinct preferences within the same receptor, indicating differential site selectivity. This suggests that under combined exposure, PAEs and their metabolites in organisms may enhance their binding capacity by targeting distinct sites, thereby amplifying their biological toxicity. Current risk assessments predominantly focus on single compounds. However, after combined action, the binding energy with ERα decreases by approximately 2 kcal/mol, while that with ERβ decreases by about 3 kcal/mol. According to similar studies, each 1 kcal/mol reduction in binding energy may correlate with a 10%-20% increase in receptor affinity [16]. Based on this calculation, the synergistic effects of metabolites may elevate toxicity risks by approximately 20%-60%. It is necessary to incorporate metabolite co-exposure into PAEs limit standards and provide new insights for designing ERα- and ERβ-targeted antagonists.

Under mixed exposure, binding strength is closely linked to receptor molecular differences. Distinct estrogen receptor subtypes exhibit specific variations: the ligand-binding cavity of ERβ is approximately 20% smaller than that of ERα, with critical amino acid substitutions (e.g., Met336 in ERβ corresponds to Leu384 in ERα), forming a more compact hydrophobic environment. These structural differences render ERβ better suited for the cooperative binding of smaller or rigid ligands (e.g., DIBP-MIBP). For instance, CNP-amino forms hydrogen bonds with Arg346 and Glu276 in ERβ, while hydrophobic interactions dominate the binding with Arg394 and Met357 in ERα. Notably, ERβ exhibits higher binding energy, likely due to its enhanced compatibility with such synergistic ligand configurations [17-18].

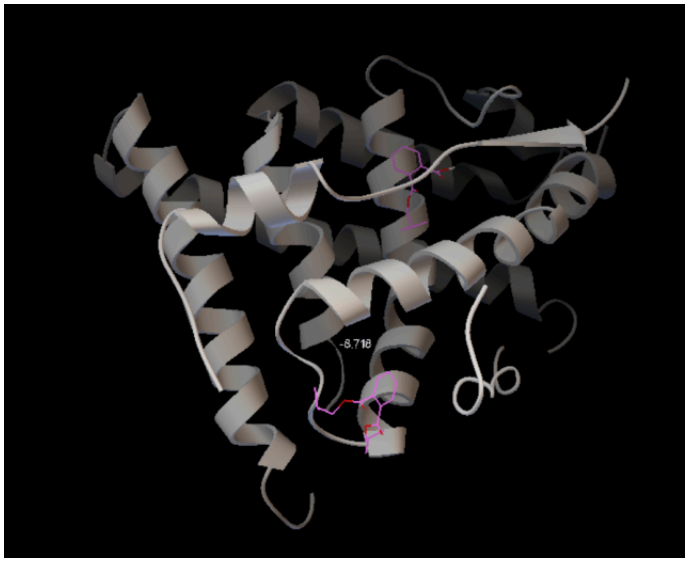

Figure 2: A case of cooperative binding with ERβ

As illustrated in Figure 2, DIBP binds to the core hydrophobic pocket of the LBD in ERβ (gray-white helical region in the figure). Its benzene ring forms π-alkyl interactions with Leu387 and Met421. Meanwhile, MIBP establishes a salt bridge through its carboxyl group with His524 (marked numerically in the figure), while its methyl side chain embeds into a hydrophobic crevice formed by Phe404 and Leu428, enhancing binding stability. The binding sites of DIBP and MIBP adopt adjacent spatial arrangements (spacing of approximately 6.6 Å), forming a "dual-ligand sandwich" conformation. Together, they induce the folding of ERβ's H12 helix (AF-2 domain) toward the

DOI: 10.54254/2755-2721/2025.GL24471

ligands, exposing the coactivator binding interface, which may amplify the receptor's transcriptional activity.

4. Conclusion

This simulation study reveals the molecular mechanisms underlying synergistic effects, demonstrating that DIBP and MIBP cooperatively activate ERα and ERβ, thereby amplifying DIBP's toxicity. These findings address gaps in previous assessments of metabolite toxicity for PAE pollutants, providing critical data to support environmental health risk evaluation, toxicity quantification of DIBP and MIBP with ERβ, revision of plasticizer usage standards, and establishment of exposure limits. However, as the experiments rely solely on static docking without accounting for solvent effects or protein conformational dynamics, further validation via molecular dynamics simulations (e.g., GROMACS) is required to strengthen the robustness of the conclusions. Additionally, the DIBP-MIBP synergy may not only enhance receptor activation through additive binding energy but also amplify toxicity by disrupting endogenous hormone homeostasis. For instance, MEHP—a metabolite of DEHP (diethylhexyl phthalate)—activates oxidative stress in the liver, elevating reactive oxygen species (ROS) and malondialdehyde (MDA) levels while suppressing superoxide dismutase (SOD) and glutathione peroxidase (GPx) activity, thereby exacerbating inflammatory damage. Since the study did not account for other biological factors affecting DIBP and MIBP in vivo, in vitro experimental validation remains essential. Given that this study does not account for such in vivo biological factors, in vitro experimental validation remains essential to confirm the observed effects and fully assess the toxicological relevance of DIBP-MIBP co-exposure. Moreover, the results provide a methodological framework for investigating whether similar synergistic mechanisms exist among other PAEs and their metabolites, thereby offering broader implications for understanding endocrine disruption and guiding future toxicological research.

Acknowledgement

Firstly, I would like to show my deepest gratitude to the professors and teaching assistants of the related courses, whose invaluable guidance and insightful feedback were instrumental in every stage of this paper. Additionally, I extend my sincere thanks to my classmates. The discussions with them significantly enriched the depth and creativity of this thesis. Further, I would like to thank all my friends and parents for their encouragement and support. Without all their enlightening instruction and impressive kindness, I could not have completed my thesis.

References

[1] Gao, H. T., Li, R. X., Di, Q. N., Gao, H. W., & Xu, Q. (2017). Exposure levels and health risks of phthalate esters in the Chinese population. Carcinogenesis, Teratogenesis & Mutagenesis, 29(6), 471-475.

[2] Cleys, P., Panneel, L., Bombeke, J., Dumitrascu, C., Malarvannan, G., Poma, G., ... & Covaci, A. (2023). Hair as an alternative matrix to assess exposure of premature neonates to phthalate and alternative plasticizers in the neonatal intensive care unit. Environmental Research, 236, 116712.

[3] Zhang, Y., Yang, Y., Tao, Y., Guo, X., Cui, Y., & Li, Z. (2023). Phthalates (PAEs) and reproductive toxicity: Hypothalamic-pituitary-gonadal (HPG) axis aspects. Journal of Hazardous Materials, 459, 132182.

[4] Zhang, Y., Yuan, Q., Jiang, M., Zheng, L., Sui, Y. M., Wang, Y. L., & Wang, C. H. (2019). Advances in toxicity and detection methods of phthalate esters. Environmental Chemistry, 38(5), 1035-1046.

[5] Li, Y. H., Lu, J. J., Yin, X. W., Liu, Z. L., Tong, Y. B., & Zhou, L. (2019). Pollution characteristics and infant health risk assessment of phthalate esters in residential environments during heating and non-heating seasons in Shihezi

DOI: 10.54254/2755-2721/2025.GL24471

City. Acta Scientiae Circumstantiae, 39(9), 3154-3162. doi: 10.13671/j.hjkxxb.2019.0162
[6] Koch, H. M., Bolt, H. M., Preuss, R., & Angerer, J. (2005). New metabolites of di (2-ethylhexyl) phthalate (DEHP) in human urine and serum after single oral doses of deuterium-labelled DEHP. Archives of toxicology, 79, 367-376.
[7] Morris, G. M., Huey, R., Lindstrom, W., Sanner, M. F., Belew, R. K., Goodsell, D. S., & Olson, A. J. (2009). AutoDock4 and AutoDockTools4: Automated docking with selective receptor flexibility. Journal of computational chemistry, 30(16), 2785-2791.
[8] Xie, Z., Zhang, X., Xie, Y., Wu, J., & Wu, Y. (2022). Occurrences and potential lipid-disrupting effects of phthalate metabolites in humpback dolphins from the South China Sea. Journal of Hazardous Materials, 439, 129939.
[9] Reinhardt Martin & Grubmüller Helmut. (2021). GROMACS implementation of free energy calculations with non-pairwise Variationally derived Intermediates. Computer Physics Communications, 264.
[10] Shi, S. F., & Yu, C. Q. (2005). Research advances in phytoestrogens and their action targets. Journal of Integrative Medicine, 3(5), 408-410.
[11] Qi, H. M. (2023). Design and implementation of an FPGA accelerator for AutoDock Vina algorithm based on low-level concurrency. (Master's thesis, Southeast University).
[12] Pu, S. Y. (2020). Toxic effects of phthalate esters on zebrafish growth, development, and glucose metabolism. (Doctoral dissertation, University of Chinese Academy of Sciences).
[13] Zhang, Y. H., Xiao, N., & Li, X. Y. (2013). Effects of endocrine disrupting chemicals on estrogen receptor signaling pathways. Journal of Shaanxi Normal University (Natural Science Edition), 41(1), 53-58.
[14] Zhou, Z., Fan, H., Yu, D., Shi, F., Li, Q., Zhang, Z., ... & Mi, W. (2023). Glutathione-responsive PROTAC for targeted degradation of ERα in breast cancer cells. Bioorganic & Medicinal Chemistry, 96, 117526.
[15] Ma, L., Wu, Y., Zhou, J., Cheng, C., Li, Y., Yao, Y., & Wu, L. (2023). Multispectral method combined with molecular modelling to investigate the binding mechanisms of DBP and DIBP on pepsin. Journal of Molecular Liquids, 390, 123090.
[16] Gao, K., Hua, K., Wang, S., Chen, X., & Zhu, T. (2025). Exploring the reproductive exposure risks of phthalates and organophosphates in atmospheric particulate matter based on quantitative structure-activity relationships and network toxicology models. Journal of Hazardous Materials, 137395.
[17] Qiu, S., Song, M. M., & Liu, C. (2023). Research advances in reproductive toxicity and molecular mechanisms of phthalates. Life Sciences, 35(7), 935-946.
[18] Zhang, Z. S., & Zhuang, S. L. (2014). Analysis of Differences in Estrogenic Effects of Chlornitrofen-amino Mediated by ERα and ERβ. Journal of Zhejiang University of Technology (Natural Science Edition), 42(3), 53-58.